



SYNTHESIS, CHARACTERIZATION AND OPTIMIZATION OF PROCESS PARAMETERS FOR COPPER DOPED ZINC OXIDE THIN FILMS

Mahammad Quayam¹, Abhinandan C. Hukkeri², Somashekhar K. Hulloli³

^{1,2,3}Asst. Professor, Department of Mechanical Engineering,
ATRIA Institute of Technology, Bangalore Karnataka,(India)

ABSTRACT

CZO thin films were synthesized by using sol-gel spin coating technique. Parameters which were considered for the study were Copper doping percentage, aging duration, Number of coating layers and post heating temperature. The structural and morphological properties were investigated using the X-ray Diffraction, Scanning Electron Microscope, Atomic force Microscope, Transmission Electron Microscope and Energy Dispersive X-ray Spectroscopy. The XRD patterns confirmed the polycrystalline nature of the films. The TEM and SEM images revealed the spherical grain morphology. Grain size of the Cu-ZnO particles was found to vary between 20 nm - 100 nm. The EDAX results show the presence of 16% of Copper content in the copper doped Zinc oxide thin films. The crystallite size was observed to decrease from 20.12 nm to 18.32 nm due to the increase in copper doping percentage in thin films. The Roughness was increased from 60.45 nm to 90.83 nm. The optimal parameters for the synthesis were found to be 3% of Cu doping percentage, 72 hrs for aging duration, 12 layers of deposition and 700^o C of post heating temperature.

Keywords: ZnO Thin Films, CZO, Sol-gel Spin coating, Structural properties.

I. INTRODUCTION

Zinc oxide (ZnO) thin films have attracted researchers because of its optical, chemical and electrical properties. ZnO comes from the group II-VI semiconductor compound having many applications in the fields of solar cells, LED, bio medical application and gas sensors etc. ZnO is an n-type semiconductor with energy band-gap of 3.37eV and high excitation binding energy of 60 MeV [1-4]. ZnO is chemically stable and non-toxic which makes it simple to fabricate for the sensor application. ZnO thin films have been widely used to monitor various harmful gases such as Hydrogen Sulfide (H₂S), Carbon Monoxide (CO) and Methane etc. Gas sensing mechanism with ZnO thin films is surface controlled where grain size and oxygen play a very significant role. One of the methods for improving gas sensing properties of thin films is by adding a finite amount of impurities such as aluminum (Al), silver (Ag) and copper (Cu) etc. Various techniques have been employed to fabricate ZnO thin films such as sol-gel spin coating [2,6,18], spray deposition, Radio frequency sputtering [5,19,20], chemical vapor deposition [7], spray pyrolysis [10] etc. The metal oxide semiconductor has been used for gas

sensing applications and there are two main difficulties such as poor selectivity of the gas and high operating temperature. This limitation can be overcome by doping suitable materials with appropriate concentration. The major purpose for doping Cu with ZnO is because Cu atoms will enhance the oxygen adsorption for the surface of the thin films which helps in decreasing the response time for gas sensing [8].

II. EXPERIMENTAL PROCEDURE

2.1 Precursor materials

The precursors used for synthesis are Zinc Acetate Dihydrate $Zn(O_2C_2H_3)_2$ as the base material, Cupric Chloride Dihydrate $[CuCl_2 \cdot 2H_2O]$ as the doping and Isopropanol $(CH_3)_2CHOH$ as the solvent, Diethanolamine was used as stabilizer for preparation of CZO thin films.

2.2 Experimental details

It's a three stage process which includes Substrate preparation, Sol preparation and film coating which are explained below in detail.

2.2.1 Substrate Preparation

Quartz substrates were cleaned in Chromic Acid to remove the impurities from its surface, then the substrates were taken into a bowl containing Acetone and the bowl was placed for 10 min in Ultrasonicator bath. Later De-ionized water used on substrates to rinse and to remove the residual impurities and then the substrates were dried in hot air oven for removing the water content [11].

2.2.2 Sol Preparation

The precursors are weighed according to the doping percentage of Cu into ZnO. For example, for 1 wt% Cu, 1:99 ratios have been used to obtain CZO. Here the Cu% which has been taken into consideration was 1, 3 and 5 wt%. All the CZO films have 0.5M percentage and to this process Diethanolamine (DEA) was added. Depending on the doping concentration the precursors and Isopropanol (IPA) were measured and poured into the Petri dish. With the help of a magnetic stirrer the solution was continuously stirred at temperature of $60^{\circ}C$ for a period of 1hr. A dark blue colored solution was obtained. To maintain the metal ion concentration 1:1 in the solution 5 ml of DEA was added. The solution was yet again stirred awaiting a homogenous solution. The sol was left for aging for a period of 24hrs and it was coated on the substrate using spin coater [12].

2.2.3 Film coating

The sols after aging are spin coated on the quartz substrate. The speed of the spinning motor was maintained at 3000 RPM and the coating duration was maintained 45 seconds for all samples. After each layer the sample were dried out in a hot air oven at $250^{\circ}C$ for 8 min for evaporating the solvent from the film. Again the substrate was coated until the desired layers were obtained (8, 12 and 16) with intermediate drying between the layers. The films are then annealed (post-deposition heat treatment) for the required temperature for phase formation ($500, 700$ and $900^{\circ}C$) for a period of 2 hrs. in a hot air oven [14-15].



III. RESULTS AND DISCUSSION

3.1 Analysis of variance (ANOVA)

3.1.1 Influence of parameters on roughness

Table 1 shows ANOVA results for the roughness of CZO film to study the contribution of each parameter. It can be observed that the Copper doping (P =39.86%) and Aging (P =25.39 %) showed significant influence on the roughness of film.

Table 1 Analysis of variance for Roughness of CZO films

Parameters	DF	SS	MS	Fcal	F0.05	P%
Cu Doping percentage	2	525.29	262.64	1.15	3.00	39.86
Aging	2	334.51	167.25	0.13	3.00	25.39
Number of deposition layers	2	79.98	39.99	0.17	3.00	6.07
Post deposition heat treatment temperature	2	148.99	74.5	0.06	3.00	11.31
Error	0					
PE	4	228.97	57.24			17.37
Total	12	1317.74	601.62			100

3.1.2 Influence of parameters on Crystallite size of CZO films

ANOVA results for crystallite size of CZO film were revealed in Table 2 to study the contribution of each parameter. It can be observed that the copper doping (37.99%) and Post heating temperature (26.43%) showed significant influence on the Crystallite size of film.

Table 2 Analysis of Variance for Crystallite size

Parameters	DF	SS	MS	Fcal	F0.05	P%
Cu Doping percentage	2	3.19	1.59	0.86	3.00	37.99
Aging	2	1.05	0.53	0.06	3.00	12.53
Number of deposition layers	2	0.08	0.04	0.02	3.00	0.97
Post deposition heat treatment temperature	2	2.22	1.06	0.13	3.00	26.43
Error	0					
PE	4	1.85	0.46			22.08
Total	12	8.39	3.69			100.00

3.1.3 Influence of parameters on Hardness of CZO films

Table 3 shows ANOVA results for the transmittance of CZO film to study the contribution of each parameter. It can be observed that the Post heating temperature (59.20%) and Layers (26.17%) showed significant influence on the Hardness of film.



Table 3 Analysis of Variance for Hardness

Parameters	DF	SS	MS	Fcal	F0.05	P%
Cu Doping percentage	2	398904	1994552	8710.98	3.00	14.38
Aging	2	6775	3377	0.00	3.00	0.24
Number of deposition layers	2	726060	363030	1585.49	3.00	26.17
Post deposition heat treatment temperature	2	1642399	821199	0.30	3.00	59.20
Error	0					
PE	4	228.97	57.24			0.01
Total	12	2774366	3182215			100

3.2. GRA of Surface Roughness, thickness and Conductivity Results

3.2.1 Data normalization

In grey relational analysis data processing is first performed in order to normalize the raw data for analysis. In this work, linear normalization of experimental results is performed in the range between zero and unity. Usually, there are three categories of performance [16-20].

Characteristics in the analysis of normalized value, i.e. the ‘Lower the better’, ‘Higher the better’ and the ‘Nominal the better’. ‘Lower the better’ and ‘Higher the better’ were considered for the percentage parameter response. Then, the normalized results can be expressed as

$$X_i^*(k) = \frac{\max X_i^* - X_i^{(0)}(k)}{\max X_i^* - \min X_i^{(0)}(k)}$$

$$X_i^*(k) = 1 - \frac{X_i^{(0)}(k) - \sigma v}{\max\{\max X_i^{(0)} - \sigma v, \sigma v - \min X_i^{(0)}(k)\}}$$

$$X_i^*(k) = \frac{X_i^{(0)}(k) - \min X_i^*(k)}{\max X_i^* - \min X_i^{(0)}(k)}$$

Where, $X_i^*(k)$ is the value after the grey relational generation, $\min X_i^{(0)}(k)$ is the smallest value of $X_i^{(0)}(k)$ for the k^{th} response, and the $\max X_i^{(0)}(k)$ is the largest value of the $X_i^{(0)}(k)$ for the k^{th} response. An ideal sequence is $X_i^*(k)$ ($k=1, 2, \dots, 9$).

The values of the all factors are set to be the reference sequence, $X_0^{(0)}(k)$, $k=1$. Moreover, the results of nine experiments were the comparability sequences $X_i^{(0)}(k)$, $i=1, 2, \dots, 9$, $k=1$.

Also, the deviation Δ_{0i} , Δ_{\max} and $\Delta_{\min}(k)$ for $i=1-9$, $k=1$ can be calculated. The deviation sequences $\Delta_{01}(1)$ can be calculated as follows:

$$\Delta_{01}(1) = |X_0^*(1) - X_1^*(k)|$$



3.2.2 Computation of grey relational coefficients

The grey relational coefficients are calculated to express the relationship between the ideal (best) and actual experimental results. The grey relational coefficient $\xi_i(k)$ can be expressed as

$$\xi_i(k) = \frac{\Delta_{\min} + \xi\Delta_{\max}}{\Delta_{0i}(k) + \xi\Delta_{\max}}$$

Where,

$\Delta_{0i} = \| X_0^*(k) - X_i^*(k) \|$ is the difference of the absolute value between $X_0^*(k)$ and $X_i^*(k)$, ξ = distinguishing coefficient between zero and one.

In this study ξ value is taken as 0.5

Δ_{\min} = smallest value of Δ_{0i}

Δ_{\max} = largest value of Δ_{0i}

Table 4 Grey relational co-efficient, grey relational grades and their order

Experiment no	Grey relation co-efficient			Grade	Order
	Roughness	Crystallite size	Hardness		
1	0.382	0.333	0.471	0.396	8
2	0.755	0.421	0.359	0.512	5
3	0.595	0.353	0.393	0.447	6
4	0.504	0.429	0.726	0.553	3
5	0.624	0.482	0.488	0.531	4
6	1.000	1.000	0.361	0.787	1
7	0.371	0.440	0.333	0.382	9
8	0.333	0.367	0.590	0.430	7
9	0.488	0.455	1.000	0.648	2

Table 5 Grey Relational grade and its order for each level

Level	Grey Relation grade	Order
A1	0.364	3
A2	0.539	1
A3	0.798	2
B1	0.604	3
B2	0.546	2
B3	0.550	1
C1	0.524	2
C2	0.595	1



C3	0.582	3
D1	0.558	2
D2	0.589	1
D3	0.554	3

The highest grade of Grey relational grading shows that the results obtained experimentally are closer to ideal optimum value. In other words, the larger the Gray relational grading, the better will be the multiple performance characteristics. Therefore, experiment 6 in the Table 4 shows the highest Grey relational grading indicating the parameter of $A_2B_3C_2D_2$ in the Orthogonal Array has the best multi performance characteristics among nine experiments. The Grey relational grading for the mean is summarized in Table 5 which shows the predicted optimal process parameter based on the Grey theory is $A_2B_3C_2D_2$ since the optimal process parameter is the combination of the levels with highest Grey relational grading.

3.3 Confirmation tests

For the concluding step the optimum level design parameters are chosen to verify the improvement in the quality using parametric level. Table 6 reveals the initial process parameter $A_2B_3C_1D_2$ experimental result for several performance features and relationship of the Grey theory prediction design $A_2B_3C_2D_2$. Results shows roughness increased from 86.34 to 90.83 nm, Crystallite size increased from 18.3 to 20.32 nm, Hardness increased from 5275.5 kg/mm² to 5325.69 kg/mm²

Table 6 Results of confirmation test for CZO thin films

Responses	Initial process parameter	Grey theory prediction design
	$A_2B_3C_1D_2$	$A_2B_3C_2D_2$
Roughness	86.34 nm	90.83 nm
Crystallite size	20.32 nm	18.3 nm
Hardness	5275.5 kg/mm ²	5325.69 kg/mm ²

3.4 Characterization Techniques

3.4.1 X Ray Diffraction (Xrd)

The crystalline structure of films was investigated by X-ray diffraction (XRD), From Fig 1 the peaks obtained clearly note that all the films are polycrystalline in nature and hexagonal wurtzite structure [21]. The CZO films indicated preferred c axis orientation perpendicular to surface of the substrate. The fig 1 (a) corresponds to experiment no 3 and it is evident that the sharp peaks with high intensities are associated at 31.69⁰, 34.37⁰, 36.19⁰, 38.03⁰, 47.38 and 56.42⁰ belongs to the miller indices (100), (002), (101), (102) and (110) respectively. Because of 1 % of Cu in ZnO films, Cu was not present in the lattice structure as the impurities. As the Cu % was increased anew intensity was obtained with 2 theta value of 39.10⁰ which was associated to (111) which belongs to Cu which is depicted in fig 1 b. As the doping percentage was increased the Cu was visible in XRD peaks.

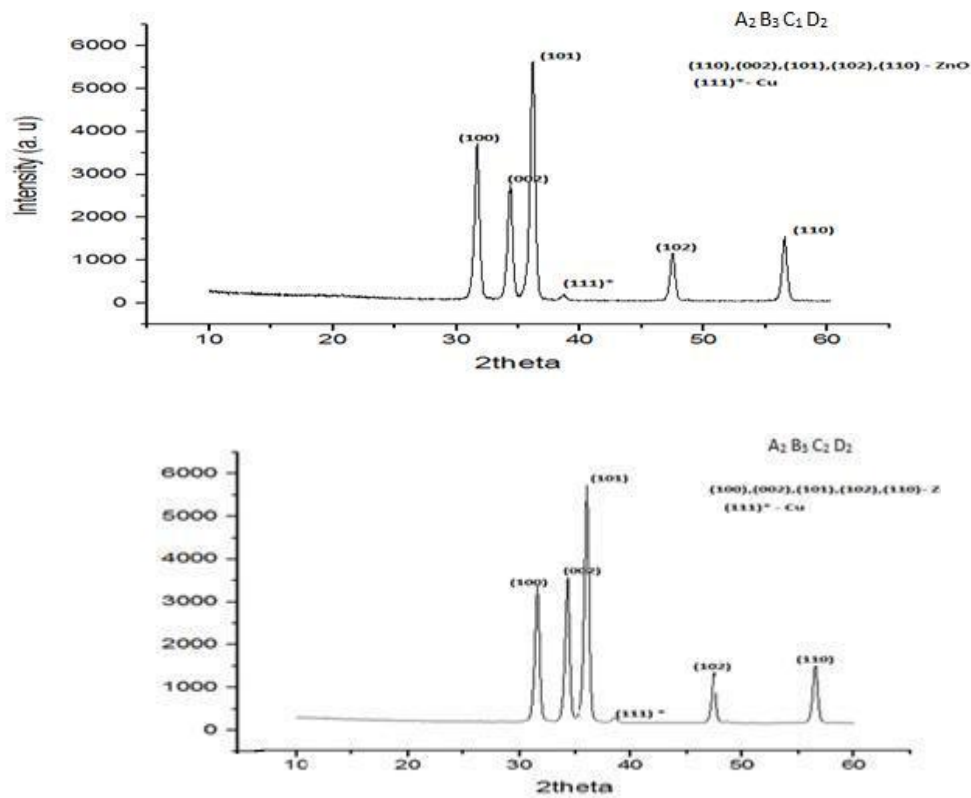


Fig 1 XRD pattern for CZO thin films

3.4.2 Scanning Electron Microscope (SEM)

It was found that the Cu doping percentage and subsequent post heating temperature influences the morphology of the surface in thin films [22]. Fig 2-a and 2-b shows uniformity in the distribution of the grain growth.

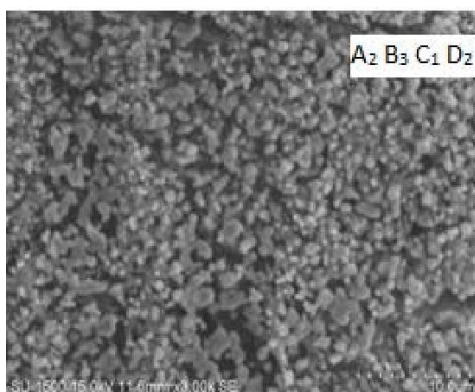


Fig 2-a

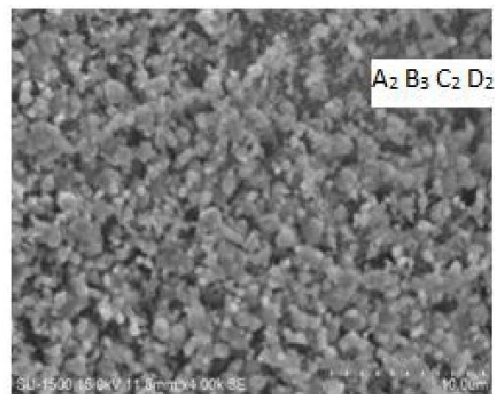


Fig 2-b

Fig 2 SEM images of CZO thin films

It was observed that the molar concentration and the annealing temperature play a significant role in formation of islands during grain formation. The grains were spherical in nature which corresponds to other Authors. The grains size for 1 % Cu doped ZnO was found to be 86 – 98 nm, grain size for 3% Cu doped ZnO was measured as 103 – 120nm, whereas for 5 % Cu doped ZnO the grain size was found to be 120-145 nm. From this data it was established that with the increase in the doping % and post-heating temperature the grain size increases. The

grain structure was dense and homogeneous in which the grains of different size was spread across the surface of the film. It was even observed that the cracks had reduced due to increase in the annealing temperature.

3.4.3 Atomic Force Microscopy (AFM)

Nanosurf with a scan speed up to 60 ms/line at 128 data point/line and scan image rotation up-to 0-360° with a maximum approach speed of 0.1 mm/s was used [23-24]. Roughness were measured by AFM which shown in 3-Dimensional Fig 3 (a) and Fig 3 (b) shows the topographic 3D images of the thin films of the various experiment. The roughness which was measured varied from 65 nm – 98 nm. The hardness was derived from the topographic data.

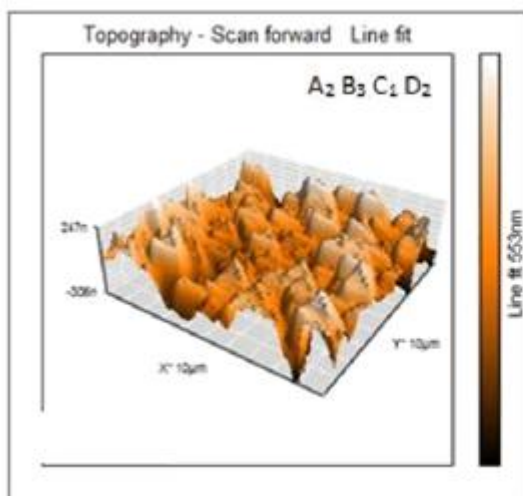


Fig.3 (a)

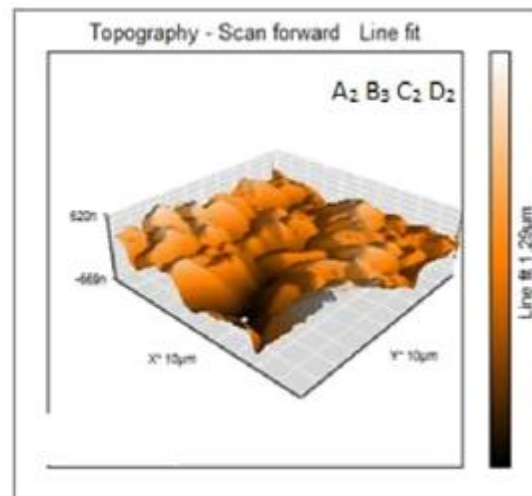


Fig.3 (b)

Fig 3 AFM images of CZO thin films

3.4.4 Transmission Electron Microscope (TEM)

The fig 4 (a) reveals the High Resolution Transmission Electron Microscope (HRTEM) image of CZO sample. The HRTEM image shows the presence of lattice fringes of average width of 0.28 nm along the particles. The average lattice spacing (d-spacing) in the TEM images confirms with the XRD results obtained for the CZO samples. As there were no visible defects, stacking faults of Cu impurities in the microstructure which shows that the Cu impurities have well incorporated into the lattice matrix of the ZnO [25]. The fig 4(b) depicts the TEM images of the particles and it was found that they were randomly arranged on the Cu Grid which was used for TEM studies. It was observed that the particles had formed clusters on the Cu grid. From the TEM images it can be confirmed that the particles were spherical in shape and the samples were having high crystallinity. The TEM image supports the SEM results as because of the presence of the similar type of the spherical structures. The particles size ranged from 20 - 100 nm throughout the Cu grid. The fig 4(c) reveals the Selected Area Electron Diffraction (SAED) of the CZO samples. The SAED pattern also clarifies that the ring patterns with the diffraction pattern spots is produced only for the polycrystalline material. The Fig 4(d) reveals the Energy Dispersive X-ray Spectroscopy (EDAX) which gives the composition of the elements in samples. Well defined peaks of the EDAX confirm the presence of the dopant Cu and precursor ZnO used initially for the preparation of the CZO samples. The elemental compositions of the samples are given in table which reveals that copper

was present.

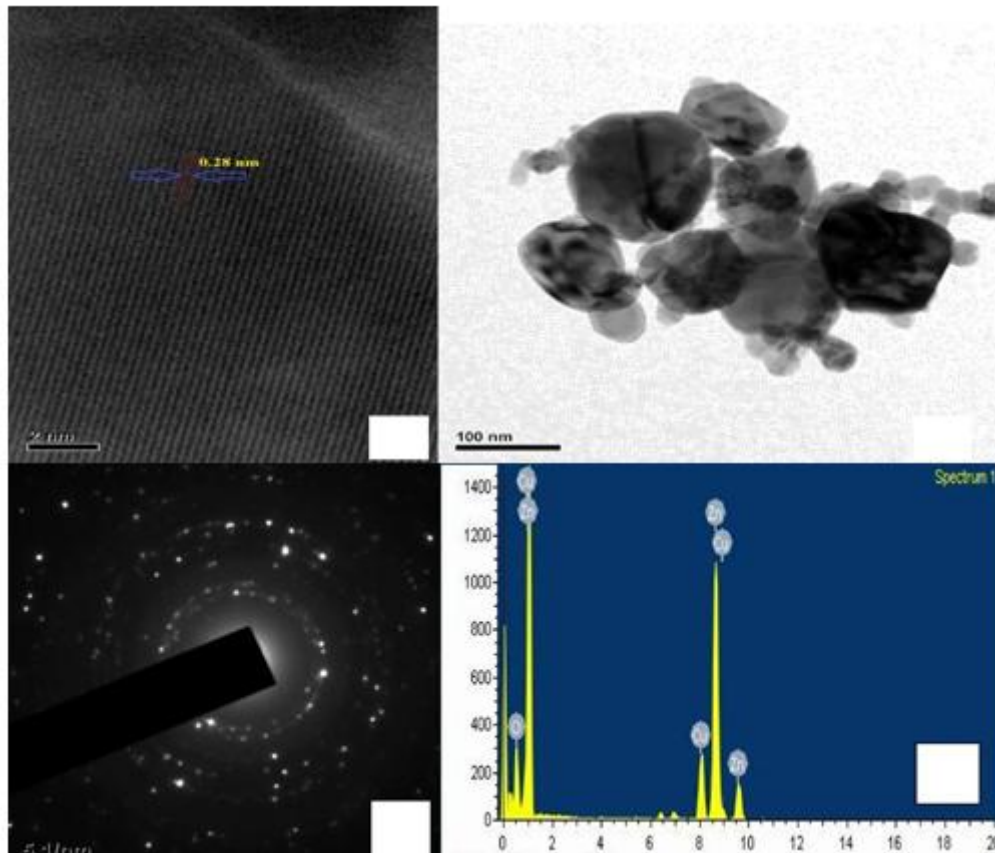


Fig 4 a) HRTEM b) TEM c) SAED d) EDAX

IV. CONCLUSIONS

Cu doped ZnO thin films were synthesized from Sol-Gel spin coating method. Crystal structure of the samples was analyzed with XRD and it confirmed that samples have hexagonal structure. Crystallite size improved due to incorporation of Cu in ZnO lattice matrix. SEM results indicate shape and size of the grain structure of the films. The TEM images depicted the particle size of the samples which varied from 20- 100 nm. The HRTEM images depicted the lattice spacing which confirms with the XRD results. The EDAX results revealed presence of Cu as impurities in lattice. Experimental studies of Roughness, Hardness and Crystallite size were tested for CZO thin films. Experimental was designed considering Doping percentage, Aging, no of layers and Post-heating temperature. Conclusions were made based on the investigated results:

- Crystalline of CZO films phase was deteriorated with increase in the Copper doping percentage and no other impurity were found which was confirmed with the SEM and TEM images.
- ANOVA results showed that Copper doping percentage was the most influencing factor with 39.86% for roughness, 37.99% for crystallite size and post deposition heat treatment temperature factor had most influence i.e. 59.20% for the Hardness.



- GRA obtained for Initial process parameter was found to be 86.34 nm for roughness, 20.3nm for crystallite size and 5275.5 kg/mm² for Hardness for films.
- The grey prediction obtained was 90.83 nm for roughness, 18.3 nm for crystallite size and 5325.69 kg/mm² for hardness.

REFERENCES

- [1] C.H.Chia, W.C.Tsai, W.C.Chou, "Preheating-temperature effect on structural and photoluminescent properties of sol-gel derived ZnO thin films", Journal of luminescence ,2014,vol. 148, pp 111-115.
- [2] Xu Liu ,Kaimeng Pan, Weibo Li,Dan Hu,Shuyang Liu,Yude Wang, "Optical and gas sensing properties of Al-doped ZnO transparent conducting films prepared by sol-gel method under different heat treatment", Ceramic international, 2014, vol 40, pp 9931-9939.
- [3] Ian Y.Y.Bu, "Effects of pre-annealing temperature on structural and optical properties of sol-gel deposited aluminium doped Zinc oxide",ceramic International,2014, vol 32, pp 779-791.
- [4] C.Y.Hsu, Y.C.Lin, L.M.Kao, Y.C.Lin, "Effect of deposition and annealing temperature on the structure and properties of Al-doped ZnO thin films", Material chemistry and Physics, 2010, vol.124, pp 330-335.
- [5] R.Mariappan, V.Ponnuswamy, P.Suresh, N. Ashok, P.Jayamurugan, A.chandra Bose, "Influence of film thickness on the properties of sprayed ZnO thin films for gas sensor applications", superlattices and Microstructures, 2014, vol.71, pp 238-249.
- [6] M.Hjiri, L.El Mir, S.G.Leonardi, A.Pistone, L.Mavilia, G.Neri, "Al-doped ZnO for highly sensitive CO gas sensors", Sensors and actuators, 2014, vol.196, pp 413-420.
- [7] P.P.Sahay, R.K.Nath, "Al-doped Zinc oxide thin films for liquid petroleum gas (LPG) sensors", Sensors and actuators, 2008, vol.133, pp 222-227.
- [8] Boubaker Benhaoua, Achour Rahal, Said Benramache, "The Structural, optical and electrical properties of nanocrystalline ZnO:Al thin films", superlattices and Microstructures, 2014, vol.68, pp 37-47.
- [9] Ahmed A, Al-Ghamdi, Omar A, Al-Hartomy, M.El Okr, A.M.Nawar, S.El-Gazzar, Farid El-Tantawy, F.Yakuphanoglu, "semiconducting properties of Al doped ZnO thin films", Molecular and Biomolecular spectroscopy,2014, vol.131, pp 512-517.
- [10] Yue Hou, Amir M, Soleimanpour, Ahalapitiya H, Jaytissa, "Low resistive aluminum doped nanocrystalline Zinc oxide for reducing gas sensor application via sol-gel process", Sensors and actuators, 2013, vol.177, pp 761-769.
- [11] M.Vishwas, K.Narasimha Rao, A.R.Phani, K.v.Arjuna Gowda, R.P.S. Chakradhar, " Optical , electrical and structural characterization of ZnO:Al thin films prepared by a low cost sol-gel method", Solid state communication, 2012, vol 152, pp 324-327.
- [12] Keh-moh Lin, Paijay Tsai, "Parametric study on preparation and characterization of ZnO:Al films by sol-gel method for solar cells", Material science and engineering, 2007, vol.139, pp 81-87.
- [13] M.sahal, B.Hartiti, A. Ridah, M.Mollar, B.Mari, "Structural , electrical and optical properties of ZnO thin film deposited by sol-gel method", Microelectronics journal, 2008, vol 39, pp 1425-1428.

- [14] V.Musat, B.Teixeira, E.Fortunato, R.C.C.Monteiro, P.Vilarinho, "Al-doped ZnO thin films by sol-gel method", surface and coating technology , 2004, vol 181, pp 659-662.
- [15] Z.Q. Xu, H.Deng, Y.Li, Q.H.Guo,Y.R.Li, "Characteristics of Al-doped C-Axis Orientation ZnO thin films prepared by sol-gel method", Material research bulletin, 2006, vol 41, pp354-358.
- [16] Jianzi Li, Jian Xu, Qingbo XU, Gang Fang, "Preparation and characterization of Al doped ZnO thin films by sol-gel process", Journal of alloys and compounds, 2012, vol 542, pp151-156.
- [17] S.W.Xue, X.T.Zu,W.G.Zheng, H.X.Deng, X.Xiang," Effect of Al doping concentration on optical paramtrers of ZnO:Al thin film by sol-gel technique", Physica,2006 , vol 381, pp209-213.
- [18] Joydip sengupta, R.K.sahoo, C.D.Mukherjee, " Effect of annealing on the structural ,topographical and optical properties of sol-gel derived ZnO and AZO thin films", Materials letters,2012, vol 83, pp 84-87.
- [19] Davood Raoufi, Taha Raoufi, "The effect of heat treatment on the physical properties of sol-gel derived ZnO thin films", Applied surface science, 2009, vol 225, pp 5812-5817.
- [20] M.H.Mamat, M.Z.sahdan,Z.khusaimi, M.Rusop, "Electrical characteristics of sol-gel Derived Aluminum Doped Zinc Oxide thin films at Different Annealing temperatures", ICEDS, 2010.
- [21] A.Ismail, M.J.Abdullah, "Effect of annealing on structural and optical Proprties of Aluminum Doped ZnO Thin Films", IEEE, 2011.
- [22] K.Schellens, B.Capon , C.De Dobbelaere, C. Detavernier, A.Hardy, M.K.Van Bael, "Solution derived ZnO:Al films with low resistivity", Thin solid Films, 2012, vol 524, pp 81-85.
- [23] Zi-Neng Ng, Kah-Yoong Chan, Thanapora Tohsophon, " Effect of annealing temperature ZnO and AZO films prepared by Sol-gel technique", Applied Surface Science,2012, Vol 258, pp 9604-9609.
- [24] C.H.Chia , W.C.Tsai, W.C.Chou, "Preheating-temperature effect on structural and photoluminescent properties of sol-gel derived ZnO thin films", Journal of Luminescence, 2014, vol 148,pp 111-115.
- [25] Vinod Kumar,Vijay Kumar, S.Som, A.Yousif, Neetu Singh, O.M.Ntwaeaborwa, Avinashi Kapoor, H.C.Swart, "Effect of annealing on the structural, morphological and photoluminescence properties of ZnO thin films prepared by Spin Coating", journal of colloid and interface Science,2014, vol 428, pp 8-15.